Fast measurements of the gas-liquid diffusion coefficient in the gaussian wake of a spherical bubble

Nicolas Dietrich[1,2,3,4]
Jessica Francois[1,2,3,4]
Mélanie Jimenez[1,2,3,4]
Arnaud Cockx[1,2,3,4]
Pascal Guiraud[1,2,3,4]
Gilles Hébrard[1,2,3,4]

[1]Université de Toulouse, INSA, LISBP, Toulouse, France.

[2]INRA, UMR792, Ingénierie des Systèmes Biologiques et des Procédés, Toulouse, France.

[3]CNRS, UMR5504, Toulouse, France.

[4]Fédération de Recherche FERMAT, CNRS, Toulouse, France.

Fast Measurements of the Gas-Liquid Diffusion Coefficient in the Gaussian Wake of a Spherical Bubble

A fast method is proposed for determining the oxygen gas-liquid diffusion coefficient from measurements of the fluorescence quenching behind a bubble. The approach consists of capturing pictures of the concentration field at micro-scale in the laminar bubble wake. The Gaussian concentration profiles measured in the wake are demonstrated to be systematically equivalent to an instantaneous plane diffusion case. The approach permits to accurately evaluate the gas-liquid diffusivity in a very short time of around one second.

Keywords: Bubble, Diffusion, Gas-liquid diffusion coefficient, Gaussian wake, Oxygen

Received: July 28, 2014; *revised*: August 26, 2014; *accepted*: February 23, 2015

DOI: 10.1002/ceat.201400471

1 Introduction

■pls. check references carefully■
Transport properties, such as conductivity, viscosity, and mass diffusion coefficients, are important in the design of chemical processes. In particular, the molecular diffusion coefficient, D, is one of the most significant physical properties to characterize the nature of molecules in solution phase from both the scientific and technological viewpoints. According to Fick's law [1], it is defined as the constant ratio of proportionality between molecular flux and concentration gradient of the species. In physical and, above all, chemical processes, the mass transfer rate is governed by convection, turbulence of flow, and molecular diffusion. Therefore, much research has been carried out on the measurement of diffusion coefficients since the first experiments on the subject [2].

The diffusion coefficient plays an important role in many processes, such as petrochemical processes, biological reactors, and waste water treatment, because it is required for the solution of the governing equations of mass transfer phenomena. Extensive research has been conducted on the diffusion coefficient over more than a hundred years, and it is well recognized that D reflects not only the molecular size or solution viscosity but also the shape of the molecule and the intermolecular interaction. Several measurement methods have been developed, e.g., the steady-state method [3], absorption measurement [4], bubble size calculation [5], interferometry [6], optical probes [7], chemical reactions [8], etc.

But classical determination methods present some limitations because of measurement by probes, intrusive and indirect technique, to which should be added hydrodynamic perturbation, natural convection, long response time, impact of the liquid media, etc. [9, 10]. Thus, available experimental data on mass diffusion coefficients are actually not sufficient because of the complications of the system and difficulties of the experimental measurements. Therefore, the objective of this study is to develop a new method for obtaining the oxygen diffusion coefficients through short-time and non-intrusive measurement in order to establish a new data base. The system uses an optical technique for accurate measurement of small transient diffusion areas. The target materials in this study are transparent solutions of several concentrations and species.

In order to contain and control the hydrodynamics, the measurement is performed in the wake of a spherical bubble. The flow in the wake of the bubble is totally controlled and occurs in the same direction z as the bubble rising velocity U_B [11]. The velocity profile V_W in the wake has a Gaussian profile given by:

$$V_w = \frac{Q_0 U_B}{4\pi\nu z} e\left(\frac{-U_B r^2}{4\nu z}\right) \quad (1)$$

where Q_0 is the wake flow rate and ν denotes the cinematic viscosity. This solution is valid far from the bubble and expresses a 2D configuration (r, z). Close to the single bubble, the potential contribution is also significant and a near-wake solution was described by Hallez and Legendre [12].

Unlike for a free gas-liquid interface plane, where natural convection occurs, this forced convection situation is perfectly controlled. Planar laser-induced fluorescence with inhibition (PLIFI) [13, 14] presents a non-intrusive alternative method. This technique is based on the addition of a fluorescent molecule absorbing light (wavelength λ_a) that re-emits an amount of the received energy (wavelength λ_f). The principle of the PLIFI technique is to illuminate a fluid containing the fluores-

Correspondence: Dr. Nicolas Dietrich (nicolas.dietrich@insa-toulouse.fr), Université de Toulouse, INSA, 135 avenue de Rangeuil, Toulouse 31000, France.

cent dye with a laser sheet and acquire images of the studied solution in the enlightened area with cameras. These molecules are called quenchers because they can inhibit the fluorescence [15–17]. It is observed that the fluorescence intensity decreases with the increase of the quencher concentration following the Stern-Volmer equation [18]:

$$\frac{I_Q}{I_0} = \frac{1}{1 + K_{SV}[Q]} \quad (2)$$

K_{SV} is the Stern-Volmer constant (L mg^{-1}), I_Q is the fluorescence intensity, and I_0 denotes this intensity in the absence of the quencher. Several works described the possibility of visualizing the oxygen concentration field [19] or in the wake of a single bubble [13–16, 20]. Qualitative measurements have been obtained for the oxygen transferred in the wake of a rising bubble [13–17, 21–27] and also for the carbon dioxide concentration map around a single bubble [21, 28].

The main limits of the PLIFI technique results from the light reflection and refraction on the bubble surfaces. A light ring is observed around the bubble, with a shadow on the side of the bubble creating a strong contrast between the both sides of the picture. Considering these results obtained in previous works, the PLIFI technique appears quite promising despite its obvious optical limitations. Some authors [14–16] proposed an alternative configuration to avoid these problems in order to follow the oxygen concentration field in the wake of bubbles. In this configuration, the laser sheet was perpendicular to the bubble trajectory and horizontal sections in the bubble wake were obtained. From these experiments, a mass transfer coefficient was calculated and a new approach is proposed to calculate fluid properties of the liquid from this alternative configuration.

2 Materials and Methods

The experimental setup displayed in Fig. 1 a comprises a transparent glass column ($0.1 \times 0.1 \times 0.3$ m^3) with a side fitted with the system of injection (1) to generate bubbles of specific sizes [29, 30]. It was composed of a thin glass capillary with a diameter of ~ 100 µm linked to a syringe pump (Harvard PHD 2000). The tank was filled with a fluid containing the fluorescent dye, i.e., the ruthenium-complex $C_{72}H_{48}N_8O_6Ru$ (Nanomeps, France) at a concentration of 30 mg L^{-1}. A laser sheet was generated (2) by a Nd:Yag laser (3) (λ_a = 532 nm, 10 Hz, 200 mJ) in the horizontal *xy* plane. As indicated in Fig. 1 b, the laser sheet is

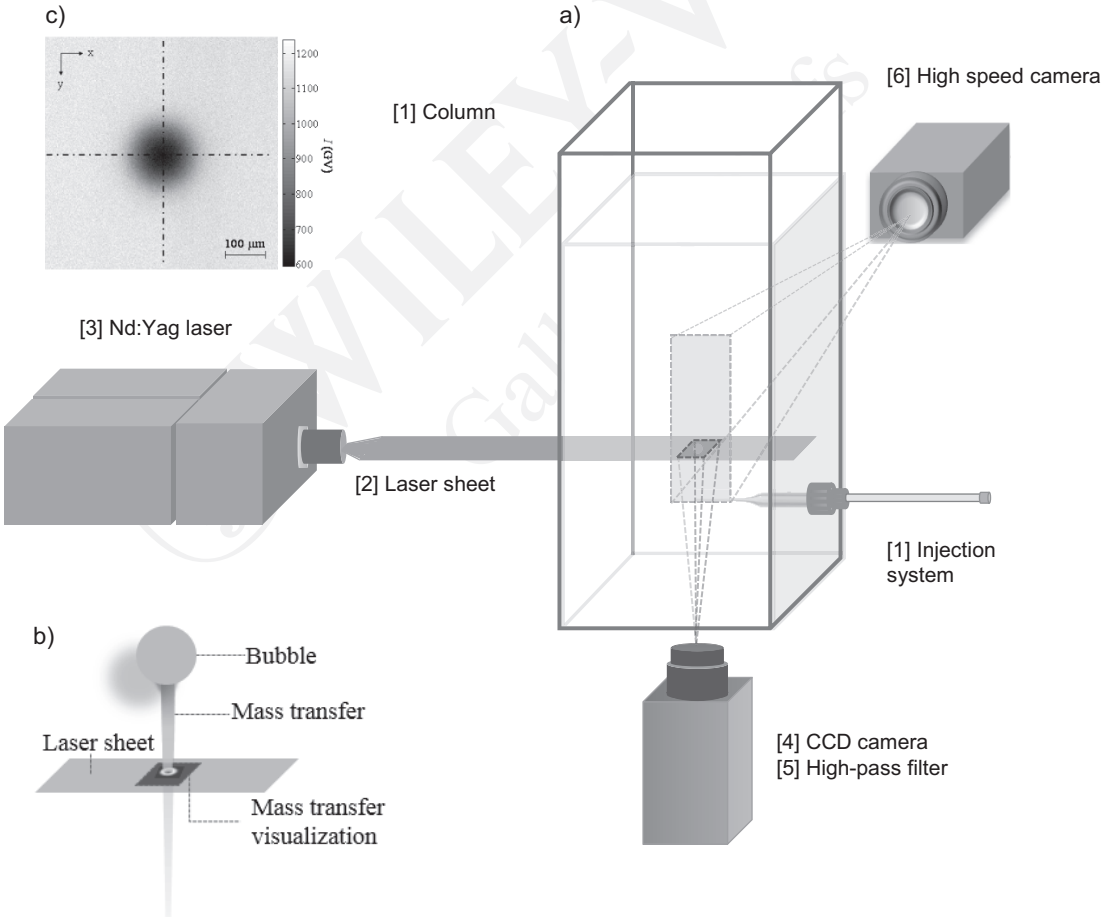

Figure 1. (a) Experimental setup. (b) Schematic representation of the bubble wake crossed by the laser sheet in the *xy* plane. (c) Raw fluorescence image expressed in gray values of a bubble wake cross section in water at $z = 3d_B$. The image corresponds to the intersection of the dashed lines in the *xy* plane in (b).

perpendicular to the bubble trajectory. A 12-bit charge-coupled device camera (4) (Imager Intense, LaVision, Germany, 10 Hz, 1040×1376 pixels^2) was placed below the column along the vertical z axis, i.e., perpendicularly to the laser plane, to acquire pictures of the fluorescence emitted by the fluid. A 105-mm objective with three teleconverters was fitted to the camera to reach a spatial resolution of 2.3 µm per pixel. In order to visualize only the fluorescence, a 570-nm high-pass filter (5) was used.

A programmable trigger unit (LaVision, Germany) synchronized the camera and the laser device. A second camera (PCO 1200, Germany, 10 bits, 770 Hz, 1024×1280 pixel^2) was placed on the lateral side (6) of the column (y axis) to record at a high frequency the bubble movement and then make possible the measurement of bubble size and bubble velocity. A 60-mm objective was fitted to this camera (55 µm per pixel).

Table 1. Hydrodynamic conditions for the six sets of experiments at 20 °C.

Experiment No.	[wt %] Glycerol	μ $\times10^{-3}$ [Pa s]	d_B [mm]	U_B [m s^{-1}]	Re	Flux $\times10^{-3}$ [g m^{-2}s^{-1}]
1	43	58	1.88	0.047	1.8	0.208
2	18	7.0	1.29	0.117	26	1.43
3	18	7.0	0.72	0.032	3.4	1.05
4	8	2.6	1.30	0.203	107	4.96
5	8	2.6	0.78	0.071	22	1.78
6	0	1.0	0.72	0.110	74	7.43

3 Results

For each experiment, the solution was previously deoxygenated with nitrogen. Then a single oxygen bubble of two sizes with $d_B \approx 1.5$ and ≈ 0.7 mm was formed in the immobile fluid. The experimental conditions are presented in Tab. 1.

Image processing of the high-speed camera images by Matlab software permits the calculation of the bubble diameter, d_B, and velocity, U_B. Then the distance z between a fluorescent recording and the position of the bubble could also be determined.

The different oxygen concentration field cross sections in the bubble wake were then recorded with the CCD camera at a frequency of 10 Hz. As an example, a raw image is displayed on Fig. 1 c. For recording, the information was originally acquired in gray values and then converted into mass concentration with the suitable calibration curve (Eq. (2)). Fig. 2 displays six superimposed elevated cross sections recorded with approximately 100 d_B distance between them. The oxygen concentration fields appear symmetric with a 3D Gaussian profile forming a concentric, rounded gradient of oxygen with the maximum concentrations at the center of the spot. In this figure, a diffusion phenomenon is discernible, with substantial flattening and widening with the time and distance far from the bubble; $t = 0$ is chosen for the first picture.

4 Discussion

The validity of the assumption of a 2D diffusion process is demonstrated by the straightness of the symmetry of the oxy-

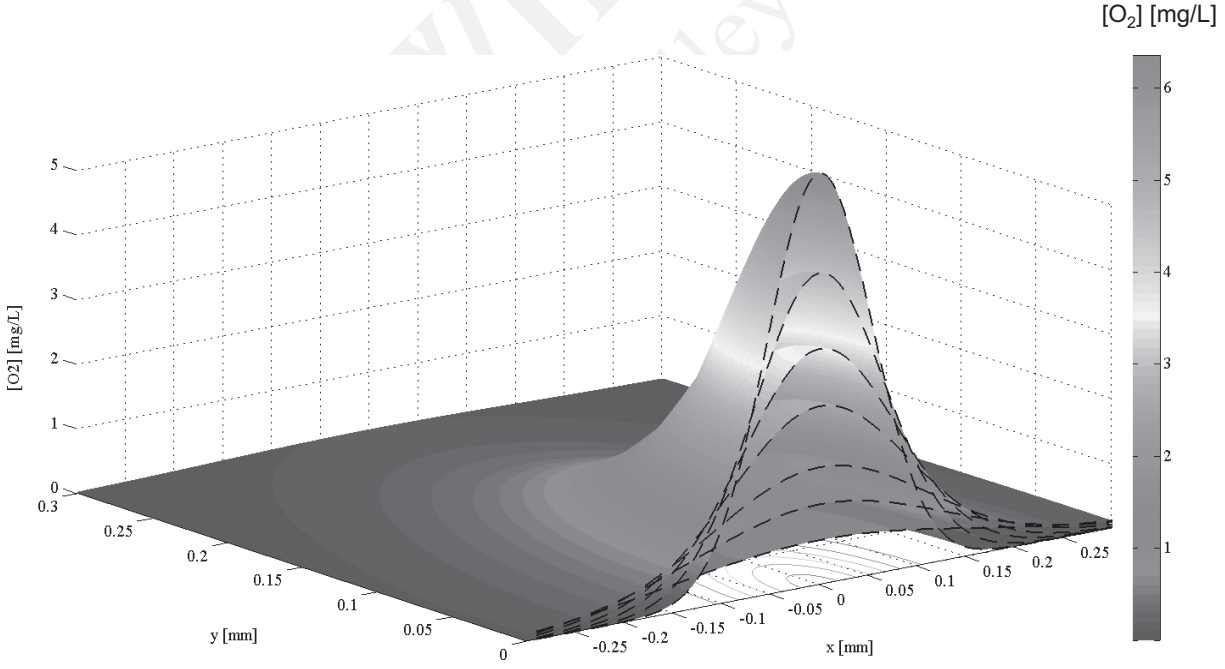

Figure 2. Elevated dissolved oxygen concentration fields in the bubble wake cross sections at $z = 3d_B$, $96d_B$, $151.8d_B$, $393.8d_B$, $449.4d_B$, and $747d_B$ (System 6).

gen spots. From these concentration fields, one can estimate the flux value calculated at successive distances z from the bubble:

$$Flux = \frac{2U_B}{{d_B}^2}\int_0^\infty [O_2] r dr \quad (3)$$

After the near wake of the bubble which is approximately equivalent to $z = 10\sqrt{\mathrm{Re}}$, the oxygen flux (Eq. (3)) becomes constant and corresponds to the total amount of mass transferred by the single bubble [15, 16]. The convection in the wake becomes essentially axial (Eq. (1)) whereas the oxygen transport is mainly radial and dominated by diffusion (Fig. 3 a). In terms of time, it corresponds to about 1–1.3 s after the bubble passage. The oxygen concentration profile $[O_2]$ is measured from the bubble wake cross-sectional images. A sample of averaged ortho-radial oxygen concentration profiles acquired at different times is plotted in Fig. 3 a. As these experimental profiles are very similar, they can be superimposed in Fig. 3 b. The dimensionless concentrations are presented versus the dimensionless radial position r/σ where σ is the standard deviation of the Gaussian equation. The graph obtained demonstrates the perfect self-similarity of the measurements which implies that the results are auto-validated and really accurate.

At $t \approx 0$, the oxygen spot always has a radius of around 100 µm. Due to the small size of the concentration field behind the bubble, i.e., around 10 % of the bubble size, it can be estimated with Oseen's equation (1) [11] that the velocity in this field can be assumed to be constant, axial, and equal to the Gaussian maximum velocity. Then, after several bubble diameters, the oxygen radial transport due to convection can be neglected as regards radial diffusion. The oxygen field in the wake is then observed to evolve as a Gaussian curve. This observation is in total agreement with the analytical solution of the Fickian diffusion equation [31]. In particular, the transient solution for an instantaneous plane source M_0 in an infinite medium is:

$$[O_2] = \frac{M_0}{4\pi Dt} e^{-\frac{r^2}{4Dt}} \quad (4)$$

where M_0 is the linear amount of substance diffusing from a Dirac point. This solution can be used far from the bubble with, $M_0 = flux/U_B$ and $4DT = 2\sigma^2$ to express the 2D concentration Gaussian profile:

$$[O_2] = \frac{Flux}{2U_B\pi\sigma^2} e^{-\frac{r^2}{2\sigma^2}} \quad (5)$$

The standard deviation of the Gaussian profile can then be defined as:

$$\sigma = \sqrt{2Dt} \quad (6)$$

This term could be measured experimentally for each oxygen spot (Fig. 3). The standard deviation σ depends on the square root of the time $\sqrt{t}$ and the slope of this function (Eq. (6)) allows for quickly calculating the diffusion coefficient corresponding to the medium under study (slope $=\sqrt{2D}$). In this method, the determination of the concentration can be dimensioned by the maximum of the concentration field in $r = 0$, $[O_2]/[O_2]_{max}$ (Fig. 3 b) and thus the liquid solubility as any calibration curve is not necessary:

$$\frac{[O_2]}{[O_2]_{max}} = e^{-\frac{r^2}{2\sigma^2}} \quad (7)$$

In the experiments, the initial ($t = 0$) standard deviation σ_0 for the first spot image varied from 67 to 85 µm. In Fig. 4, the ordinate axis has been translated by $\Delta\sigma = \sigma - \sigma_0 = \Delta\sigma = \sqrt{2Dt}$ to allow the comparison between experiments. A very clear linear trend can be observed for all the systems, with a regression linearity coefficient of less than 1 %, confirming the applicability of the diffusion model of Eq. (4). The slope of the curve increases as the viscosity decreases. The diffusion coefficient was quantified in six hydrodynamic conditions representing four different media. The oxygen diffusion coefficients obtained in liquid media are reported in Tab. 2. Firstly, the oxygen diffusion coefficient measured in clean water at 20 °C and $D_{water} = 2.09\times10^{-9}\ m^2s^{-1}$, is in agreement with the mean value of $2.14\times10^{-9}\ m^2s^{-1}$ found in the literature [32–34].

The reduction in viscosity with decreasing concentrations of glycerol is mainly responsible for increasing diffusion coefficients (Tab. 1). This is explained as the usual dependency of D on the inverse of the viscosity, as predicted by the Stokes-Einstein-Sutherland equation [35] and the correlation of [36]. For all water-glycerol mixtures, the latter correlation gives values very close to the obtained experimental results with a deviation of < 2.24 %.

The reproducibility of the experiments was also tested by reiterating the same measurement five

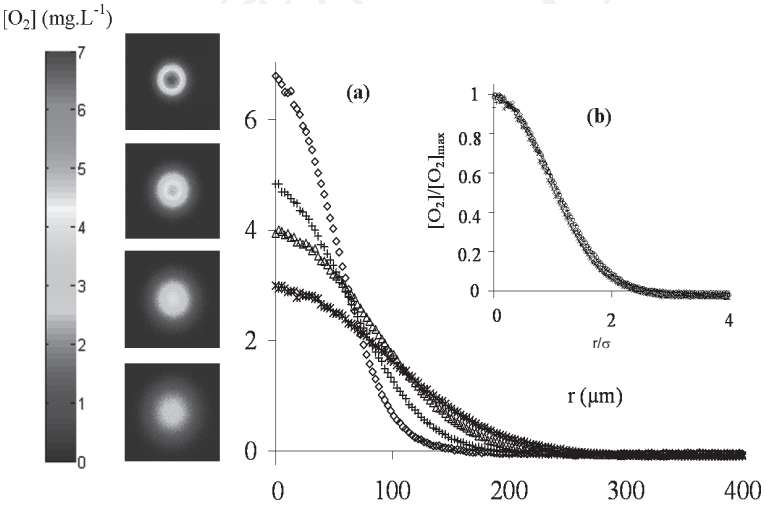

Figure 3. (a) Radial $[O_2]$ profiles at $z = 3d_B$, $96d_B$, $189d_B$, $282d_B$ (System 6). (b) Self-similarity curve for $[O_2]/[O_2]_{max}$ for the System 6 experiments.

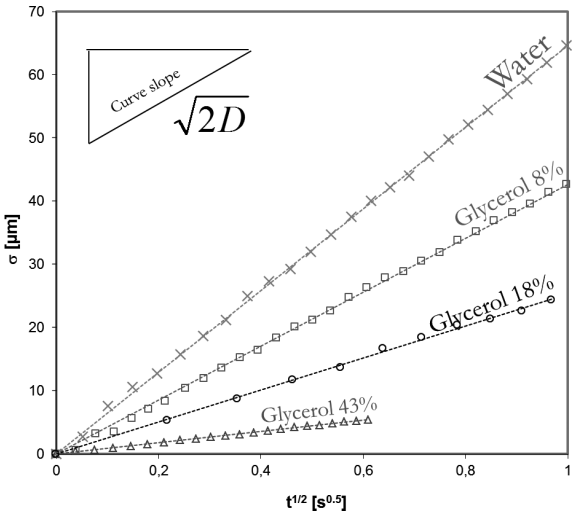

Figure 4. Variation of the standard deviation Gaussian spot *s* with Ö*t*.

Table 2. Hydrodynamic conditions for the six sets of experiments at 20 °C.

Experiment No.	Glycerol [wt %]	$D_{measured}$ [$m^2 s^{-1}$]	$D_{Literature}$ [$m^2 s^{-1}$] [36]
1	43	3.97×10^{-11}	4.03×10^{-11}
2	18	3.22×10^{-10}	3.21×10^{-10}
3	18	3.26×10^{-10}	3.21×10^{-10}
4	8	9.03×10^{-10}	9.19×10^{-10}
5	8	9.15×10^{-10}	9.19×10^{-10}
6	0	2.09×10^{-9}	2.14×10^{-9}

times under identical operating conditions. The deviation of the measured diffusion coefficient was of the order of 3 %. For two concentrations of glycerol, i.e., 8 and 18 wt %, the experiments were performed for two different sizes of bubbles, namely, 0.7 and 1.3 mm. The diffusion coefficient varied by less than 1 % between the two bubble sizes. Even though the initial sizes of the oxygen spots $r_{i,0}$ were quite different, their time evolution depended only on diffusive transport. In particular, Eq. (4) is the solution for a point source $r_{i,0} = 0$. This equation is then applicable whatever the bubble size (0.7–1.88 mm) as long as the experimental configuration can be assumed to be axisymmetric and without any radial convection. All these results clearly validate the magnitude of the experimental quantitative measurements.

The essential feature of the present method is that the measurement is accomplished in a very short time within a few seconds. The time necessary for the diffusion spot to reach the bubble size is estimated from Eq. (6) as $t = d_B^2/16D$. The accuracy is high with less than 2 % and the measurement needs to be achieved at microscale (diffusion area $<< d_B^2$). Another important feature of the proposed method is that the influence of saturation concentration on the calculation of D is eliminated due to the measurement of the Gaussian curve standard deviation versus time. As the molecular diffusion ($m^2 s^{-1}$) depends only on the spread of the spot, any calibration for concentration is necessary. A possible source of error in the present experiment arises from the temperature control in the experimental process. The experimental system was placed in a specially designed working space, where the room temperature was controlled by an air conditioner. Moreover, the diffusion can be considered as a constant temperature process since the experiment is completed within a very short time period of ~ 1 s. This is also one of the advantages of the present method over other methods requiring long measurement times.

5 Conclusions

The approach developed here uses PLIFI as an interesting optical configuration for diffusion quantification of an oxygen spot created by a single bubble rising in viscous fluids. The determination of the diffusion coefficient only requires knowledge of the oxygen spots in a cross section in the bubble wake as a function of time. The diffusion coefficient from classical established theories and the experimental values obtained in this study are in a good agreement, demonstrating the relevance of this method. Application of the technique to different transparent fluids could extend the current data and so become a useful tool for diffusion analysis and visualization.

The authors have declared no conflict of interest.

References

[1] A. Fick, *Ann. Phys. Chem.* **1855**, *170*, 59–86.
[2] T. Graham, *Q. J. Sci.* **1829**, 27.
[3] M. J. Tham, K. K. Bhatia, K. F. Gubbins, *Chem. Eng. Sci.* **1967**, *22*, 309–311.
[4] H. Sovová, J. Procházka, *Chem. Eng. Sci.* **1976**, *31*, 1091–1097.
[5] W. J. De Blok, J. M. H. Fortuin, *Chem. Eng. Sci.* **1981**, *36*, 1687–1694.
[6] Z. Guo, S. Maruyama, A. Komiya, *J. Phys. Appl. Phys.* **1999**, *32*, 995–999.
[7] W. J. Bowyer, W. Xu, J. N. Demas, *Anal. Chem.* **2004**, *76*, 4374–4378.
[8] M. Jamnongwong, K. Loubiere, N. Dietrich, G. Hébrard, *Chem. Eng. J.* **2010**, *165*, 758–768.
[9] D. A. Blackadder, J. S. Keniry, *J. Appl. Polym. Sci.* **1973**, *17*, 351–363.
[10] D. A. Blackadder, J. S. Keniry, *J. Appl. Polym. Sci.* **1974**, *18*, 699–708.
[11] C. W. Oseen, *Astron. Och Fys.* **1910**, *6*, 29.
[12] Y. Hallez, D. Legendre, *J. Fluid Mech.* **2011**, *673*, 406–431.
[13] M. Jimenez, N. Dietrich, A. Cockx, G. Hébrard, *AIChE J.* **2013**, *59 (1)*, 325–333.
[14] M. Jimenez, N. Dietrich, G. Hébrard, *Chem. Eng. Sci.* **2013**, *100*, 160–171.
[15] J. François, N. Dietrich, P. Guiraud, A. Cockx, *Chem. Eng. Sci.* **2011**, *66 (14)*, 3328–3338.

[16] J. François, N. Dietrich, A. Cockx, *Mod. Phys. Lett. B* **2011**, *25 (5)*, 1993–2011.
[17] A. Dani, P. Guiraud, A. Cockx, *Chem. Eng. Sci.* **2007**, *62*, 7245–7252.
[18] O. Stern, M. Volmer, *Phys. Zeitschr.* **1919**, *20*, 183–188.
[19] G. Herlina, G. H. Jirka, *Exp. Fluids* **2004**, *37*, 341–34.
[20] M. Jimenez, N. Dietrich, G. Hébrard, *Mod. Phys. Lett. B* **2012**, *26 (6)*, ■pages?■.
[21] S. Someya, S. Bando, Y. Song, B. Chen, M. Nishio, *Int. J. Heat Mass Transfer* **2005**, *48*, 2508–2515.
[22] O. Bork, M. Schlueter, N. Raebiger, *Can. J. Chem. Eng.* **2005**, *83*, 658–666.
[23] S. Roy, S. R. Duke, *Rev. Sci. Instrum.* **2000**, *71*, 3494.
[24] S. Roy, S. R. Duke, *Exp. Fluids* **2004**, *36*, 654–662.
[25] A. Kerbeche, J. Milnes, N. Dietrich, G. Hébrard, B. Lekhlif, *Chem. Eng. Sci.* **2013**, *100*, 515–528.
[26] N. Dietrich, K. Loubière, C. Gourdon, G. Hébrard, *Chem. Eng. Sci.* **2013**, *100*, 172–182.
[27] M. Jimenez, N. Dietrich, J. R. Grace, G. Hébrard, *Water Res.* **2014**, *58*, 111–121.
[28] M. Stöhr, J. Schanze, A. Khalili, *Exp. Fluids* **2009**, *47*, 135–143.
[29] N. Dietrich, N. Mayoufi, S. Poncin, N. Midoux, H. Z. Li, *Chem. Pap.* **2013**, *67 (3)*, 313–325.
[30] N. Dietrich, N. Mayoufi, S. Poncin, N. Midoux, H. Z. Li, *Chem. Eng. Sci.* **2013**, *92*, 118–125.
[31] J. Crank, *The Mathematics of Diffusion*, Oxford University Press, New York **1975**.
[32] C. O. Bennett, I. J. E. Momentum, *Heat and Mass Transfer*, McGraw-Hill, New York **1967**.
[33] R. Perry, D. W. Green, *Perry's Chemical Engineer's Handbook*, McGraw-Hill, New York **1997**.
[34] E. G. Scheibel, *Ind. Eng. Chem.* **1954**, *46*, 2007.
[35] A. Einstein, *Ann. Phys.* **1905**, *17*, 549–560.
[36] C. R. Wilke, P. Chang, *AIChE J.* **1955**, *1*, 264–270.

Communication: Since literature data on mass diffusion coefficients are actually not sufficient, a fast method is proposed to obtain oxygen diffusion coefficients from measuring the fluorescence quenching behind a bubble. Planar laser-induced fluorescence with inhibition presents a non-intrusive alternative method to accurately evaluate the gas-liquid diffusivity in a very short time.

Fast Measurements of the Gas-Liquid Diffusion Coefficient in the Gaussian Wake of a Spherical Bubble

N. Dietrich*, J. Francois, M. Jimenez, A. Cockx, P. Guiraud, G. Hébrard

Chem. Eng. Technol. **2015**, *38 (XX)*, XXX … XXX

DOI: 10.1002/ceat.201400471